05

Parameters of stimulated emission in $Al_{0.65}Ga_{0.35}N:Si/AlN/Al_2O_3$-structure with planar geometry

© P.A. Bokhan[1], K.S. Zhuravlev[1], Dm.E. Zakrevsky[1,2], T.V. Malin[1], N.V. Fateev[1,3]

[1] Rzhanov Institute of Semiconductor Physics, Siberian Branch, Russian Academy of Sciences, Novosibirsk, Russia
[2] Novosibirsk State Technical University, Novosibirsk, Russia
[3] Novosibirsk State University, Novosibirsk, Russia

e-mail: fateev@isp.nsc.ru

Received August 09, 2024
Revised September 30, 2024
Accepted September 30, 2024

The parameters of stimulated emission from the $Al_{0.65}Ga_{0.35}N/AlN/Al_2O_3$-heterostructure were experimentally studied in the wide spectral range of 370−670 nm at room temperature, caused by the action of transverse pulsed optical pumping with the wavelength radiation of 266 nm, pulse duration of 8 ns, and the repetition rate of the 10 Hz. The silicon doped $n_{Si} \approx 1.5 \cdot 10^{20}\,cm^{-3}$ film of the concentration $Al_{0.65}Ga_{0.35}N$, with a thickness of 1.1 μm is the asymmetric planar with the optical gain of $\sim 10\,cm^{-1}$. The quantum efficiency of stimulated emission is $\eta \approx 18\%$ at the optical pumping power of the $P_p = 100\,kW/cm^2$ and the output of stimulated emission through the Al2O3 substrate. The emission spectrum consists of a set of equidistant peaks, each of which consists of the sum of two plane TE and TM waves. These waves propagate in a zigzag manner due to internal reflection at the boundaries of the structure. A narrow angular divergence of 5.3° of stimulated emission in the direction perpendicular to the plane of the structure is obtained, and the parallel direction divergence is 20°.

Keywords: heavily doped $Al_xGa_{1-x}N$ structures, planar waveguide, optical gain, donor−acceptor recombination.

DOI: 10.61011/EOS.2024.09.60040.6977-24

1. Introduction

Wide-band $Al_xGa_{1-x}N$-structures are the promising materials in optical electronics for creation of light sources in UV-band of the spectrum [1]. Extensive doping with Si in concentration $n_{Si} > 10^{19}\,cm^{-3}$ of layers $Al_xGa_{1-x}N$ with $x > 0.5$ leads to formation of effective radiative recombination centers with high internal quantum yield of luminescence $\eta \geq 0.5$ [2]. The structures emit a broadband spectrum with $\lambda = 350-750$ nm and keep their luminescent properties up to temperature of 400°C. This makes it possible to create broadband light-emitting sources and narrow-line lasers with a wavelength tuning in the entire visible spectral range of the spectrum for a single emitting element. The wide-band emission of radiation primarily occurs in a visible range of spectrum due to a donor−acceptor recombination with a radiative recombination cross-section of $\sim 10^{-15}\,cm^2$ at maximal concentration of the recombination centers of over$10^{20}\,cm^{-3}$ [3]. Earlier, in study [4] experimentally was obtained a stimulated emission of radiation with an inhomogeneous broadened contour within $\lambda = 380-700$ nm, which protruded from the structure perpendicularly towards the end of $Al_{0.68}Ga_{0.32}N$-film, at that the portion of the transformed pumping energy into the stimulated emission energy was $\sim 7\%$.

Despite the fact that the internal quantum yield of luminescence of the studied structures is high [2], the external luminescence efficiency is significantly lower, since due to the high refractive index n , most of the emission is fully internally reflected from all surfaces, after which it is absorbed in the medium. Accordingly, only that small fraction of the radiation passes through the surface, which falls on it at an angle $\Theta \leq \arcsin(1/n)$. At $n \approx 2.19$ [5] angle $\Theta < 27°$. The use of an optical cavity matched with the excitation region may enhance efficiency of luminescence energy transformation into a stimulated emission considerably. In a laser optical cavity, the emission amplification has a propagation direction perpendicular to the emitting surface. However, due to a large gain factor that takes place in the studied structures which are planar waveguides themselves the emission mainly propagates through zigzag waveguide modes.

In the study [6], planar waveguides based on amorphous silicon carbide films of submicron thickness deposited on a quartz substrate were studied. When the photoluminescence was excited by green emission with $\lambda = 532$ nm (2-d harmonic of Nd:YAG-laser) in the outgoing modes of the emitting spectra the short spikes of the linearly (TE- and TM-) polarized emission were recorded. It was demonstrated that emission wavelength is practically independent on the grazing angles of emission outgoing from the substrate. In paper [7], it was experimentally shown that a layer of silicon nanocrystals created by implantation of silicon ions into a synthetic silicon wafer

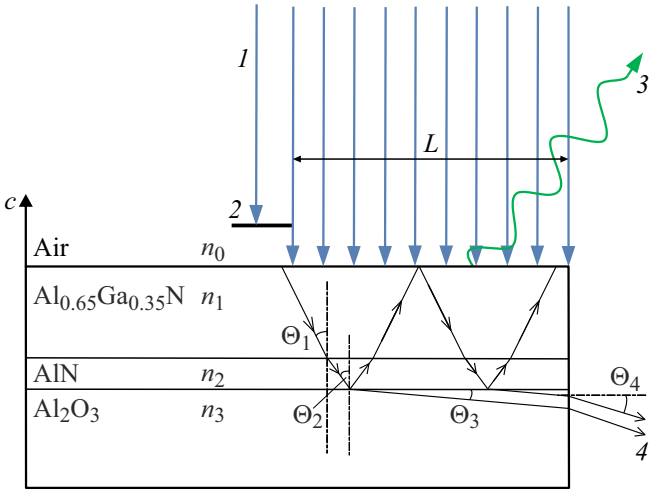

Figure 1. Diagram of excitation and recording of outgoing emission of $Al_{0.65}Ga_{0.35}N/AlN/Al_2O_3$-heterostructure: *1* — optical pumping, *2* — diaphragm, *3* — luminescence, *4* — stimulated emission of radiation.

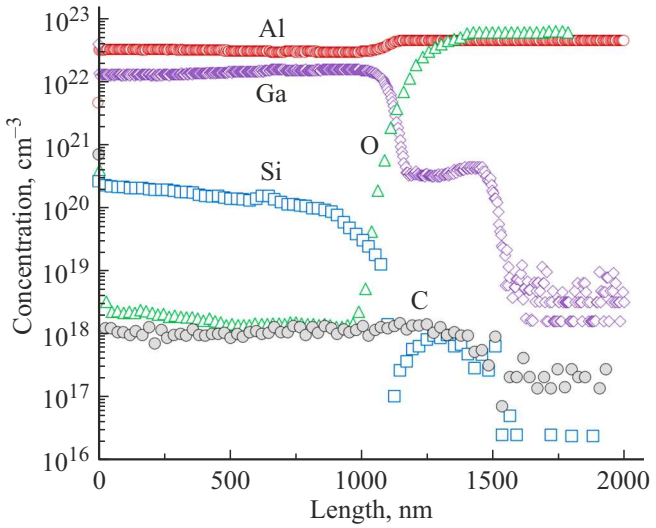

Figure 2. SIMS-analysis of $Al_{0.65}Ga_{0.35}N/AlN/Al_2O_3$-heterostructure.

forms a single-mode planar optical waveguide. It is shown that directional transverse electric and transverse magnetic modes are formed in such a waveguide from the nanocrystals' broad photoluminescent emission, which leads to a significantly narrower emission spectrum for these modes. In study [8] optical gain coefficients were measured and stimulated emission of radiation within the range $\lambda = 650-900$ nm was obtained.

The heavily-doped $Al_{0.65}Ga_{0.35}N$:Si-structure with a buffer AlN-film on sapphire substrate represents itself a planar waveguide. Emission was outgoing from it through the boundary separating$Al_{0.65}Ga_{0.35}N$:Si-film and sapphire substrate due to the walk-off modes. The purpose of this paper is to experimentally study the parameters of stimulated emission during optical pumping with $\lambda = 266$ nm for the effective removal of stimulated emission energy from the structure and for improvement of the outgoing emission geometry.

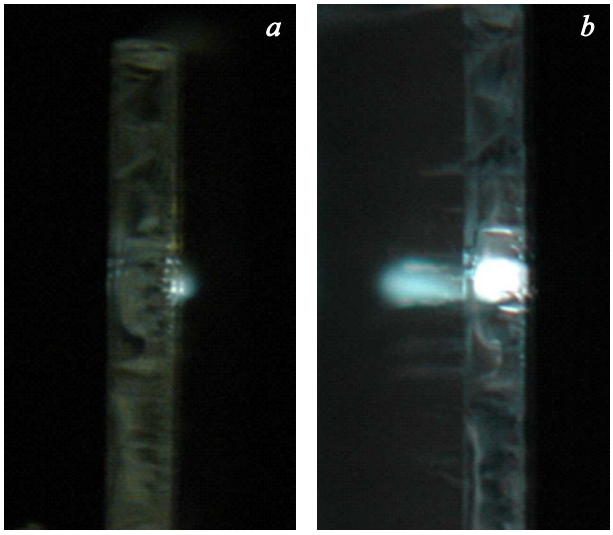

Figure 3. Photos of a transverse cleavage of $Al_{0.65}Ga_{0.35}N/AlN/Al_2O_3$-heterostructure under transverse optical pumping: (*a*) cleavage surface is perpendicular to the recording direction, (*b*) cleavage surface is inclined at an angle of $\sim 12^\circ$ to the recording direction. The intensity of optical pumping slightly exceeds the threshold for stimulated emission of radiation.

2. Technique and experimental results

The investigated $Al_{0.65}Ga_{0.35}N/AlN/Al_2O_3$-heterostructure (Fig. 1) consists of an active layer of $Al_{0.65}Ga_{0.35}N$ $h_0 \approx 1.1\,\mu$m thick with a buffer layer of AlN $h_1 \approx 360$ nm thick grown on (0001) oriented nitrided sapphire substrates Al_2O_3 with a thickness of $h = 430\,\mu$m and represents itself an asymmetrical planar waveguide [9]. Technology of $Al_{0.65}Ga_{0.35}N$ films synthesis and measurement of their parameters are described in details in [10]. The molecular-beam epitaxy method was used to grow the films. Ammonia with a flow of 130 cm^3/min was used as a source of active Nitrogen. A mixture of silane ($\sim 0.7\%$) and nitrogen with permanent gas mixture flow ~ 3 cm^3/min was used as a source of impurity (doping) silicon atoms.

The distributions of concentrations of silicon, aluminum, gallium, oxygen, and carbon atoms across the depth of the heterostructure as obtained by secondary ion mass spectrometry (SIMS) are shown in Fig. 2. With concentration of silicon $n_{Si} \approx 1.5 \cdot 10^{20}$ cm^{-3} in $Al_{0.65}Ga_{0.35}N$ films the conductivity is practically absent. Investigation of $Al_{0.65}Ga_{0.35}N$ film surface morphology by method of atomic-force microscopy demonstrates a smooth surface with a root-mean-square roughness of < 4.7 nm, and < 1 nm for the sapphire surface. All the studied

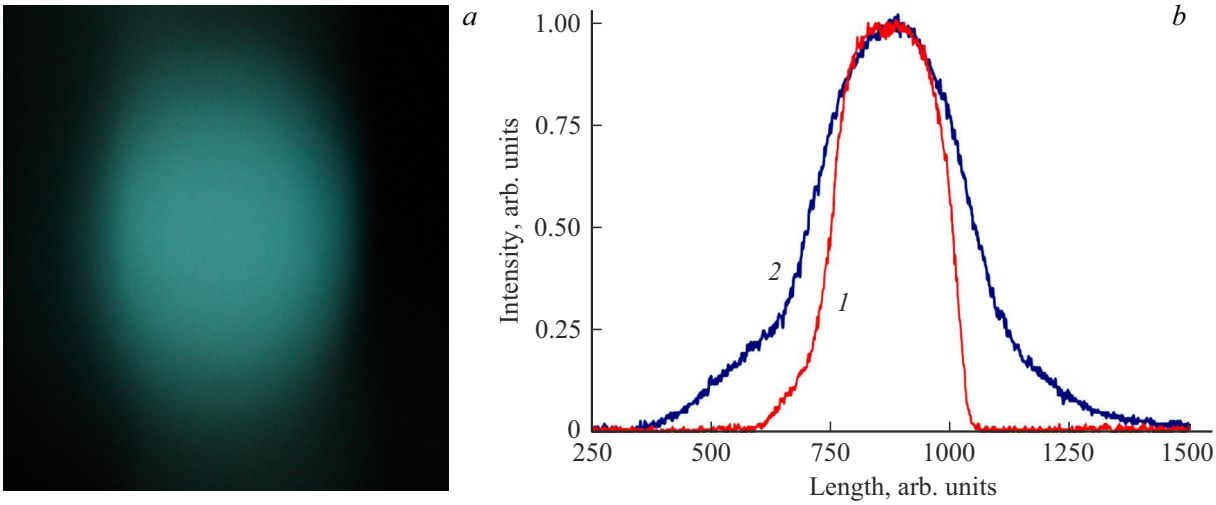

Figure 4. (*a*) Photo of the output spot of the stimulated emission. (*b*) Spatial distribution of the outgoing beam intensity for two mutually perpendicular directions: *1* — horizontal (perpendicular to the structure surface), *2* — vertical (along the surface structure).

samples were obtained by chipping the structures along the crystallographic planes of sapphire. Photos of the transverse cleavage for $Al_{0.65}Ga_{0.35}N/AlN/Al_2O_3$-heterostructure are shown in Fig. 3.

The emitting properties were studied under optical excitation from the side of $Al_{0.65}Ga_{0.35}N$-film by emission of the fourth harmonic of a pulsed Nd : YAG laser with $\lambda = 266$ nm with a pulse duration at half maximum of 8 ns and repetition rate of 10 Hz. All experiments were performed at room temperature. The pumping emission, which passed through a cylindrical lens with a focal length of 8 cm was directed perpendicular to the sample surface and consisted of a uniform strip with a width of $b = 280\,\mu$m and an excitation zone length of $L = 0-1$cm with an adjustable spacing of $5\,\mu$m. At that, estimates based on absorption coefficients show that $\sim 50\%$ of the incident pumping emission on the structure surface is absorbed in $Al_{0.65}Ga_{0.35}N$-film [3]. Maximum pulse power density on the sample surface without destroying it reaches $P_p \approx 9\,\text{kW/cm}^2$. The inhomogeneity of the pumping emission intensity along the pumping band was less than 5%.

The luminescence parameters were measured at an angle of about 45° to the sample plane, and the stimulated emission — from the end of the structure from the sapphire substrate at an angle of 11.4° (Fig. 1), at which the maximum emission intensity was observed. The spectra were measured by a spectrometer in a dynamic range of $\lambda = 250-800$ nm and spectral resolution of 0.5 nm [11]. The polarization characteristics of the output emission were studied using a polarizer — Glan prism. Part of the emission intensity measurements were carried out at a fixed wavelength using a prism monochromator with a resolution of 10 nm and a photomultiplier FEU−106, the electrical signal from which was recorded by oscilloscope Tektronix TDS2024B. Then emission was transmitted to the spectrometer and monochromator via the quartz optical fiber waveguide with a diameter of 0.1 cm. The absolute values of the pumping power and stimulated emission of radiation were measured by sensor Thorlabs S401C.

The absolute values of the gain coefficients in $Al_{0.65}Ga_{0.35}N$-film were obtained earlier intensity [3] by direct measurement of sample emission intensity gain in the presence of optical pumping. With the pumping power density of $P_p = 100\,\text{kW/cm}^2$ in the center of the emission line with $\lambda_0 = 500.7$ nm the value was for the gain coefficient $k \approx 1830\,\text{cm}^{-1}$ was obtained. In studies [12,13] to measure the optical intensification a single-pass measurement method was used — emission intensity $I(\lambda_0, L)$ from the heterostructure edge versus length of the intensified region L:

$$I(\lambda_0, L) = \big(I_s s/k(\lambda_0)\big)\big(\exp[(k(\lambda_0) - a)L] - 1\big), \qquad (1)$$

where a — loss factor if emission propagated inside the film, I_s — power density of spontaneous emission, s — cross-sectional area of the excited region.

The emergence of stimulated emission was determined by an exponential increase in luminescence intensity with an increase in the length of the excitation zone L, or by the intensity of pumping, as well as by the formation of the spectrum mode structure and output emission spot with low divergence. In our case, there is no narrowing of the emission line width, since the luminescence spectrum is characterized by inhomogeneous broadening of the emission line associated with the predominant mechanism of donor-acceptor recombination [3].

Figure 4 shows a photo of a spot of stimulated emission at a distance of 15 cm from the emitting structure, as well as the intensity distribution for two mutually perpendicular directions. These results demonstrate a homogeneous nature of distribution, close to the Gaussian distribution. Figure 5 shows the results of measuring the angular divergence of stimulated emission from the end of a sapphire

substrate for the two mutually perpendicular directions: — curve *1* with $\Delta\alpha = 5.3°$ in perpendicular and curve *2* with $\Delta\alpha = 19.5°$ in parallel directions to the surface of the heterostructure, where $\Delta\alpha$ — angle for half of the amplitude of the stimulated emission intensity.

Figure 6 shows characteristic luminescence spectra measured at the same optical pumping power density $P_p = 100\,\text{kW/cm}^2$; stimulated emission spectra containing intensified components observed at the detection angle $\alpha = -11.4°$ from the normal to the cleaved sapphire end; stimulated emission spectra measured at two polarizer positions (parallel and perpendicular to the surface of the heterostructure), which show different emission frequencies of spectral components for emission with two various polarization parameters.

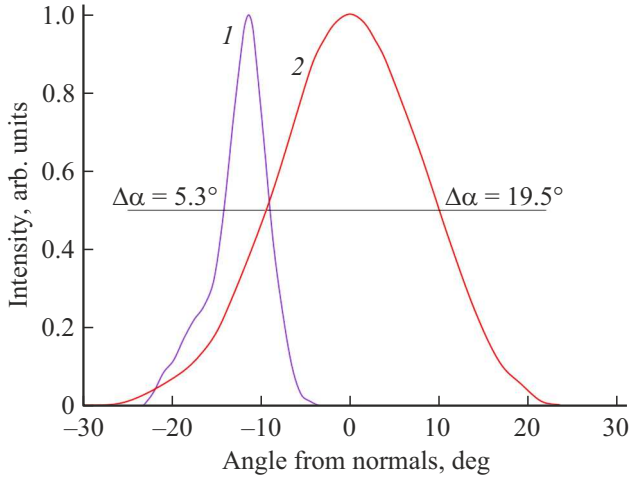

Figure 5. Angular divergence for the stimulated emission intensity as a function of the angle from normal to the cleavage surface at the pumping power density of $P_p = 100\,\text{kW/cm}^2$: *1* — horizontal divergence (the waveguide input edge is scanned along the axis *c* (Fig. 1), *2* — vertical divergence (scanning direction is perpendicular to the axis *c* (Fig. 1).

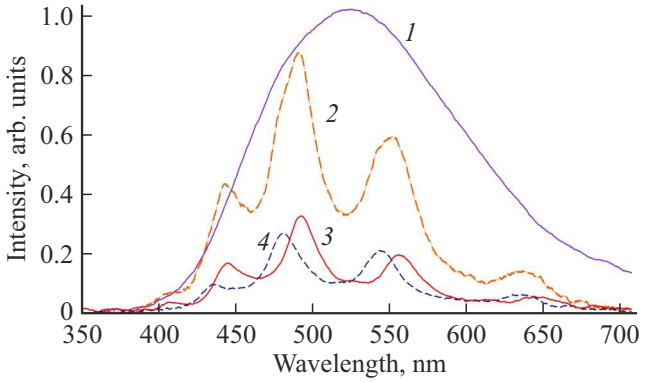

Figure 6. Emission spectra of $Al_{0.65}Ga_{0.35}N/AlN/Al_2O_3$-heterostructure with the density of the optical pumping power $P_p = 100\,\text{kW/cm}^2$: *1* — luminescence, *2* — stimulated emission of radiation, *3* — TM-mode, *4* — TE-mode of stimulated emission of radiation.

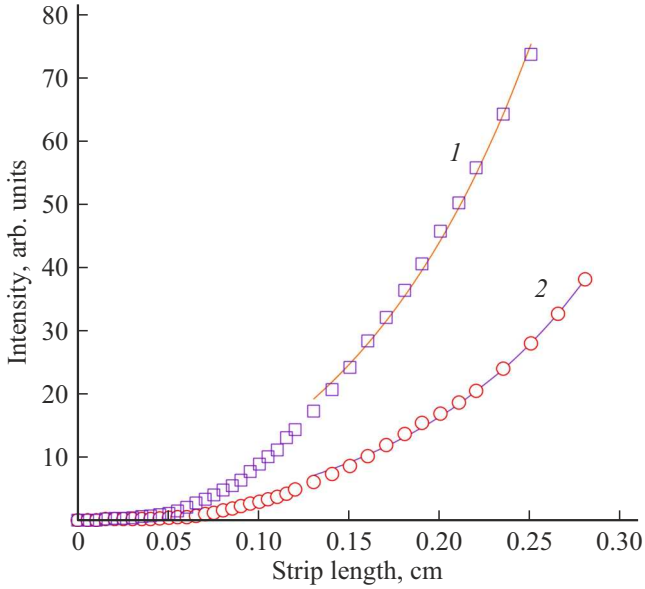

Figure 7. Stimulated emission intensity as functions of the excitation stripe length *L* with optical pumping power density of $P_p = 100\,\text{kW/cm}^2$: *1* — emission intensity obtained through integration of full spectrum *2* — emission intensity at wavelength of $\lambda_0 = 488\,\text{nm}$. Solid lines — interpolation of experimental data by the formula (1).

Fig. 7 shows dependencies of the stimulated emission intensity at one optical pumping power $P_p = 100\,\text{kW/cm}^2$ on the length of the excitation stripe *L*: integral (curve *1*) and spectrum component with $\lambda_0 = 488\,\text{nm}$ (curve *2*). Both dependences are characterized by the presence of a generation threshold and a change from linear to nonlinear. The optical gain with emission propagation in $Al_{0.65}Ga_{0.35}N$-film proves exponential behavior of curves at large values *L*. Calculations using formula (1) give the same optical gain coefficients $k \approx 9.3\,\text{cm}^{-1}$ for both experimental curves.

Experimental dependences of the stimulated emission intensity on the pump power density for $L = 0.5$ and 2 mm (Fig. 8) also demonstrate threshold behavior, which confirms the occurrence of stimulated emission at the pump power density of $P_p > 5\,\text{kW/cm}^2$.

Quantum efficiency of the pumping energy transformation at power density of $P_p = 100\,\text{kW/cm}^2$ into the energy of stimulated efficiency made $\eta \approx 18\%$, which exceeds the earlier obtained value in paper [4].

3. Discussion of the results

Parameters of stimulated emission are determined mainly by the optical properties of the excited medium. In the studied sample $Al_{0.65}Ga_{0.35}N/AlN/Al_2O_3$-heterostructure was used consisting of $Al_{0.65}Ga_{0.35}N$ film with refractive index $n_1 \approx 2.17$ [5], buffer layer AlN with $n_2 \approx 2.08$ [5] and sapphire substrate with $n_3 \approx 1.776$ [14]. Outer surfaces of the structure contact with air with $n_0 = 1$. In this case

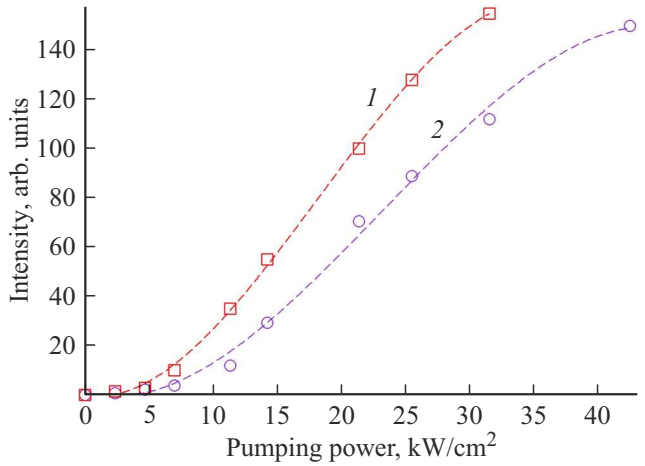

Figure 8. Curves of stimulated emission versus pumping power density: *1* — $L = 2$ mm, *2* — $L = 0.5$ mm.

$n_1 > n_2 > n_3 > n_0$, and, hence, there exist several critical incident angles of emission Θ onto the interface of the contacting media (Fig. 1) [15]. Emission outgoing from any point inside $Al_{0.65}Ga_{0.35}N$-film has a full internal reflectance at incident angles exceeding some critical angle. At the interface $Al_{0.65}Ga_{0.35}N-$air is $\Theta_1 = \arcsin(n_0/n_1)$. Calculations using Fresnel equation [15] show that reflectance at the interface of $Al_{0.65}Ga_{0.35}N$ film and buffer layer AlN is small because of small difference between the refractive indices of contacting media ($\sim 0.14\%$). Additionally, the film thickness $h_1 \approx 360$ nm is less than the luminescence wavelength. As a result emission from $Al_{0.65}Ga_{0.35}N$-film efficiently permeates into AlN-layer and therefore, the region with $Al_{0.65}Ga_{0.35}N$ film and buffer AlN-layer may be considered as a single waveguide and the generated emission is fully reflected internally at the incident angles of over $\Theta_2 = \arcsin(n_3/n_1)$.

For three major peaks in the spectrum of stimulated emission (Fig. 6) with wavelengths of $\lambda_1 = 441.8$ nm, $\lambda_2 = 488.6$ nm and $\lambda_3 = 547.8$ nm using equation for the full internal reflectance angles and refraction indices for $Al_{0.65}Ga_{0.35}N$-film $n_1 = 2.19$, 2.17, 2.15 [5] and for sapphire $n_3 = 1.781$, 1.776, 1.770 [14] it is possible to obtain critical angles, respectively $\Theta_1 = 27.3°$, 27.4°, 27.7° and $\Theta_2 = 54.83°$, 54.93°, 55.41°. At the incident angles less than Θ_1 and Θ_2 at the interfaces $Al_{0.65}Ga_{0.35}N-$air and $Al_{0.65}Ga_{0.35}N-$sapphire the emission will pass through these interfaces. The value of the emission propagation angle in $\Theta_{2\,exp}$ structure can be calculated using Snell formula from the experimentally measured angle corresponding to the maximum intensity of stimulated emission outgoing from $\Theta_4 = 11.4°$ structure (Fig. 5). For $\lambda_1 = 441.8$ nm, $\lambda_2 = 488.6$ nm and $\lambda_3 = 547.8$ nm we obtain experimental values $\Theta_{2\,exp} = 54.04°$, 54.44° and 54.9°. The obtained values $\Theta_{2\,exp}$ are lower than values for critical angles Θ_2 by 0.79°, 0.49° and 0.57° , respectively. Due to this, the emission from $Al_{0.65}Ga_{0.35}N$-film may permeate into the sapphire substrate because of refraction at the Interface of the film and sapphire substrate.

Position of the equidistant peaks recorded in the experimental spectra (Fig. 6) is explained by the model presented in jcite9. The light field in a planar waveguide may be represented as a sum of two flat TE- and TM-waves. These waves propagate in the structure as in a planar waveguide due to internal reflection at the boundaries of the structure. For a light wave propagating in a dielectric layer, in addition to internal reflectance, the phase matching condition shall be satisfied after two reflections from the upper and lower surfaces of the waveguide layer(„in one zigzag“):

$$2kn_1h\cos\Theta + \delta_1 + \delta_2 = 2\pi m, \qquad (2)$$

where $k = 2\pi/\lambda$ — wavenumber, h — waveguide thickness, δ_1 and δ_2 — phase shifts at full internal reflectance at the waveguide boundary, m — integer number defining the order of the mode. Since the propagation of an electromagnetic wave in a waveguide is resonant, only certain waveguide modes can propagate in a certain type of waveguide. Each type of mode is characterized by its spatial field distribution in the transverse direction, polarization, etc. Depending on the ratio of the refractive indices, as well as the angle of incidence of the light wave at the interface, the wave can either channel into the waveguide layer or exit into the substrate.

Equation (2) allows finding the distance between modes and wavelengths based on the known parameters of the waveguide. Phase shifts δ_1 and δ_2 under full internal reflectance may be found by Fresnel equation [15], which due to their small value may be neglected. From the experimentally determined angles $\Theta_{2\,exp}$ using formula (2) we may calculate the thickness h of $Al_{0.65}Ga_{0.35}N$ film. From calculations we may see that the film thickness for $\lambda_{1,2,3}$ within the measurements accuracy has the same value of $h \approx 1.55\,\mu$m which exceeds the value $h \approx 1.1\,\mu$m obtained from analysis of the structure using SIMS method (Fig. 2). Such an increase in thickness of the waveguide layer is largely due to the Goos–Henchen effect [9].

Additionally, the formation of the spectrum in the intensifying medium is influenced by the condition under which the maxima of stimulated emission occur at the wavelengths at which the greatest intensification takes place. Under the condition of homogeneous pumping along the excitation zone, the greatest gain is realized on such waveguide modes, for which the gain after two reflections from the upper and lower surfaces of the waveguide layer $G = \exp(2kh/\cos\Theta)$ reaches the largest value. Since k is constant in length, in the case of propagation in the gain medium along a zigzag path with internal reflectance, the value of G is determined by the angle of Θ. The greatest gain is achieved at the values of the angle $\Theta \geq \Theta_2$, when there is a complete internal reflectance in the planar waveguide.

If condition $\Theta < \Theta_2$ is satisfied, there's no full internal reflectance from the waveguide walls and the emission exits the waveguide through $Al_{0.65}Ga_{0.35}N/Al_2O_3$ interface. As

the angle decreases Θ , the fraction of emission walking off the waveguide increases due to refraction at the boundary, while the gain decreases.

The experimental data obtained are consistent with the proposed waveguide model described by the formula (2). Spectral position of peaks in the emission spectrum of $\lambda_{1,2,3} \approx 441.8$, 488.6 and 547.8 nm (Fig. 6) corresponds to $m = 9$, 8 and 7 with the film thickness of $h \approx 1.55\,\mu$m. For higher or lower λ there occurs a phase mismatch at full internal reflectance which leads to higher losses and weakens or suppresses the super-emission (provided $\Delta\lambda_{1/2} \ll \lambda$, where $\Delta\lambda_{1/2}$ — half-width of the emission line).

Polarization measurements of the outgoing emission showed the presence of two groups of differently polarized peaks with different spectral positions. A similar situation arises from the coexistence of two TE and TTM modes with perpendicular polarization and different phase shifts in the waveguide. The difference in the spectral position of TE and TM polarization bands is determined by the difference in refractive indices for different polarizations and the different reflection conditions at the boundaries.

The accuracy of determining the angles of incidence near critical angles does not allow estimating the energy of emission penetrating the substrate. Data calculated using Fresnel equation shows the fraction of the refracted energy at a level of $\sim 50\%$. As a result, the overall emission gain is significantly reduced when zigzag components propagate in the film, since they are intensified in only two passes, since a significant part of the energy flows into the substrate. Therefore, the gain of the test signal measured in one pass $k = 1830\,\text{cm}^{-1}$ [4] decreases to the value $(k-a) \approx 9.3\,\text{cm}^{-1}$ with zigzag propagation in the film, taking into account losses. It is also necessary to take into account the loss of emission during propagation in the film due to the heterogeneity of its boundaries. Inside the waveguide, as well as at the interface with the substrate and the coating medium, optical inhomogeneities exist in any waveguide (grain boundaries, pores, regions with a different phase composition of the material, optical surface imperfections, and etc.). A light beam of a waveguide mode, falling, for example, into the region of the inhomogeneity localization, will be scattered on it.

The penetration of emission from the film into the substrate can also occur due to the transition layer. In this case, this is AlN-film which interfaces with the sapphire substrate. As shown from SIMS-analysis from Fig. 2, thickness of this area is about 300 nm. Therefore, the physical interface between the two media has a transition layer and never looks like a geometric plane. In the presence of such a layer, the reflectance laws become more complicated compared to Fresnel's equation, which properly describe experimental results for monochromatic homogeneous waves. Real broadband electromagnetic waves, as in the present case, are unstable, spatially inhomogeneous, which leads to a violation of the law of internal reflectance near the critical angle [16,17].

4. Conclusion

The obtained results evidence of a possibility to use the heavily-doped $Al_{0.65}Ga_{0.35}N:Si/AlN/Al_2O_3$-heterostructure as an active medium in a wide range of the visible light spectrum which may serve the basis for further development of diode lasers.

All obtained results indicate the stimulated nature of emission with a small divergence. One of the important points in the creation of new laser sources is the study of the amplification behavior of the active medium. The measured gain coefficients $k \approx 10\,\text{cm}^{-1}$ in a planar waveguide demonstrate that they may be promising in further development of the broadband stimulated emitters in the visible light spectrum.

Funding

The study has been performed under the state assignment. FWGW−2022−0012.

Conflict of interest

The authors declare that they have no conflict of interest.

References

[1] R. Xu, Q. Kang, Y. Zhang, X. Zhang. Micromachines, **14**, 844 (2023). DOI: 10.3390/mi14040844
[2] P.A. Bokhan, N.V. Fateev, T.V. Malin, I.V. Osinnykh, Dm.E. Zakrevsky, K.S. Zhuravlev. J. Lumin., **203**, 127 (2018). DOI: 10.1016/j.jlumin.2018.06.034
[3] P.A. Bokhan, K.S. Zhuravlev, D.E. Zakrevsky, T.V. Malin, N.V. Fateev. FTP, **57** (9), 49 (2023) (in Russian). DOI: 10.61011/FTP.2023.09.56987.5627
[4] P.A. Bokhan, K.S. Zhuravlev, Dm.E. Zakrevsky, T.V. Malin, I.V. Osinnykh, N.V. Fateev. FTP, **56** (12), 594 (2022). DOI: 0.21883/FTP.2022.12.54511.4349
[5] D. Brunner, H. Angerer, E. Bustarret, F. Freudenberg, R. Hopler, R. Dimitrov, O. Ambacher, M. Stutzmann. J. Appl. Phys., **82**, 5090 (1997). DOI: 10.1063/1.366309
[6] A.V. Medvedev, A.A. Dukin, N.A. Feoktistov, V.G. Golubev. ZhTF (in Russian) **86** (5), 118 (2016). DOI: 10.1134/S1063784216050169
[7] J. Valenta, I. Pelant, K. Luterova, R. Tomasiunas, S. Cheylan, R.G. Elliman, J. Linnros, B. Honerlage. Appl. Phys. Lett., **82** (6), 955 (2003). DOI: 10.1063/1.1544433
[8] K. Luterova, D. Navarro, M. Cazzanelli, T. Ostatnicky, J. Valenta, S. Cheylan, I. Pelant, L. Pavesi. Phys. Stat. Sol. C, **2** (9), 3429 (2005). DOI 10.1002/pssc.200461206
[9] H. Kogelnik. IEEE Trans. Microwave Theory Tech., **23** (1), 2 (1975). DOI: 10.1109/TMTT.1975.1128500
[10] K.S. Zhuravlev, I.V. Osinnykh, D.Y. Protasov, T.V. Malin, V.Yu. Davydov, A.N. Smirnov, R.N. Kyutt, A.V. Spirina, V.I. Solomonov. Phys. Stat. Sol. C, **10**, 315 (2013). DOI: 10.1002/pssc.201200703
[11] B.M. Ayupov, I.A. Zarubin, V.A. Labusov, V.S. Sulyaeva, V.R. Shayapov. J. Opt. Technol., **78**, 350 (2011). DOI: 10.1364/JOT.78.000350

[12] K.L. Shaklee, R.E. Nahory, R.F. Leheny. J. Lumin., **7**, 284 (1973). DOI: 10.1016/0022- 2313(73)90072-0
[13] A. Oster, G. Erbert, H. Wenzel. Electron. Lett., **33**, 864 (1997). DOI: 10.1049/el:19970605
[14] I.H. Malitson. JOSA, **52**, 1377 (1962).
[15] M. Born, E. Wolf. *Principles of Optics* (Pergamon Press, Oxford, 1975). DOI: 10.1016/0030-3992(75)90061-4
[16] P.D. Kukharchik, V.M. Serduyk, I.A. Titovitsky. ZhTF (in Russian) **69** (4), 74 (1999).
[17] A.P. Sviridov. Quantum Electron., **37** (1), 1 (2007)(in Russian). DOI: 10.1070/QE2007v037n01ABEH013309

Translated by T.Zorina